AIAA 98-3693

Shot-By-Shot Erosion Modeling Of Retired 120mm M256 Gun Tube #1988

S. Sopok, P. Vottis, P. O'Hara, G. Pflegl, C. Rickard
US Army ARDEC-Benet Labs
Watervliet, NY

34th AIAA/ASME/SAE/ASEE
Joint Propulsion Conference & Exhibit
July 13-15, 1998 / Cleveland, OH

(34th AIAA Joint Propulsion Meeting, Cleveland, 13-15 July 1998)

SHOT-BY-SHOT EROSION MODELING OF RETIRED 120MM M256 GUN TUBE #1988

Samuel Sopok, Patrick Vottis, Peter O'Hara, George Pflegl, Christopher Rickard
US Army Benet Laboratories,
Watervliet, New York 12189

ABSTRACT

As our gun erosion database increases for in-service and out-of-service 120mm M256 tubes with M829Ax series rounds, distinct erosion patterns and mechanisms are emerging. Variability exists for M256 guns with M829Ax series rounds depending on round count, round type, round conditioning temperature, and their order. Our Materials Ablation Conduction Erosion (MACE) M256/M829A2 gun system erosion model, with its interior ballistics, thermochemistry, and boundary layer components, is constantly being refined by this erosion data. A recent refinement includes the improvement of the gun steel subsurface exposure model due to high quality-difficult to obtain data from in-service M256 tubes. Another recent refinement includes the improvement-incorporation of case gas laminar cooling-turbuluent mixing effects and forcing cone induced vena contracta effects into the boundary layer heat transfer model based on thermal data from M256 tubes. This second refinement is calibrated as a function of axial position by chromium-plate-recrystallization and gun steel-transformation temperature depths. A comprehensive gun erosion model is described for the 120mm M256 gun with its M829Ax series rounds. In addition, a detailed shot-by-shot erosion modeling prediction is described for retired 120mm M256 gun tube serial number 1988. For this gun tube, the erosion prediction includes the two types of rounds fired (M829, M829A2) and the three conditioning temperatures for each round (hot, ambient, cold). The gun erosion mechanism consists of heat checking of the inert chromium plate, subsequent interfacial degradation of the subsurface gun steel substrate at the chromium crack bases, subsequent chromium platelet spalling, and subsequent bare gun steel gas wash. This gun erosion model correctly predicts that the worst eroded region (3 mm deep) is at 1.2 – 2.4 meters RFT and that the excessive muzzle wear (chromium loss without gun steel gas wash) is by a different purely mechanical mechanism.

INTRODUCTION

The existence of thermal-chemical-mechanical gun barrel erosion is documented in US Army reports[1]. Numerous ADPA Tri-Service sponsored gun erosion meetings have implied a thermal-chemical-mechanical gun barrel erosion mechanism[2]. A unified computer model for predicting thermal-chemical-mechanical erosion in gun barrels was first described by Dunn and Sopok in 1995 using the MABL boundary layer, CCET thermochemistry, and MACE materials ablation conduction erosion gun codes[3]. This gun barrel erosion model requires XNOVAKTC interior ballistics gun code input[4]. To the degree available, our practical approach to gun barrel erosion modeling is kept on-track with actual experimental gun system data. As our gun erosion database increases, our gun erosion model evolves to include identifiable patterns.

The purpose of this paper is to describe our comprehensive gun erosion model for the 120mm M256 gun with its M829Ax series rounds. In addition, a detailed shot-by-shot erosion modeling prediction is described for retired 120mm M256 gun tube serial number 1988. For this gun tube, the erosion prediction includes the two types of rounds fired (M829, M829A2) and the three conditioning temperatures for each round (hot, ambient, cold).

PROCEDURE

A comprehensive gun erosion model was developed for the 120mm M256 gun with its M829Ax series rounds. Many types of experimental data were used to keep this gun erosion model on-track. These data include: 1) pressure gauge and radar data for

XNOVAKTC as well as 1320 K chromium plate recrystallization temperature depth and 1000 K gun steel transformation temperature depth data for MABL. These data also include kinetic rate function and subsurface metallographic data for CCET as well as borescope, subsurface metallographic, 1320 K chromium plate recrystallization temperature depth, and 1000 K gun steel transformation depth data for MACE.

Initial 120mm M256 gun tube serial number 1988 gun system erosion modeling includes XNOVAKTC interior ballistic analyses for gas pressure, gas temperature, and gas velocity core flow data at the hot (49 C), ambient (21 C), and cold (-32 C) round conditioning temperatures[4]. This initial step is followed by respective MABL boundary layer recovery enthalpy-cold wall heat flux analyses and the respective CCET thermochemistry inert wall enthalpy-reacting wall enthalpy-ablation potential analyses[3]. Final tube #1988 gun system erosion modeling includes respective MACE material ablation conduction erosion temperature profiles-wall erosion profile analyses[3]. Specifically, a detailed shot-by-shot erosion modeling prediction is described for this retired gun tube. This erosion prediction includes the two types of rounds fired (M829, M829A2) and the three conditioning temperatures for each round (hot, ambient, cold).

RESULTS AND DISCUSSION

For 120mm M256 gun tube serial number 1988, Figure 1 summarizes the XNOVAKTC interior ballistic analyses for maximum values of gas pressure (Pg), gas temperature (Tg), and gas velocity (Vg) for its M829 and M829A2 rounds as a function of axial position and round conditioning temperature. Selected axial positions include 0.69, 1.55, 2.18, 3.30, and 5.11 meters from the rear face of the tube (RFT) while the selected round conditioning includes the hot (49 C), ambient (21 C), and cold (-31 C) temperatures. Experimental pressure-time and muzzle velocity data are used to calibrate these interior ballistic analyses which are the starting point for the overall erosion modeling analysis providing input to all subsequent modules. In Figure 1, the Tg and Pg values decrease with increasing axial position while the Vg values increase with increasing axial position for the bore region.

For M256 gun tube #1988, Figure 2 summarizes the M829 and M829A2 MABL mass addition to boundary layer analyses for maximum values of recovery enthalpy (Hr) and cold wall heat flux (Qcw) as a function of axial position and round conditioning temperature. Selected axial positions and round conditioning temperatures are the same as those used in Figure 1. In Figure 2, the Hr and Qcw values increase with increasing axial position for the 0.6-1.2 meter RFT region, both values peak in the 1.2-2.4 meter range, then both values decrease with increasing axial position to the muzzle. This deviation in Figure 2 from the core flow pattern in Figure 1 is explained by an improved boundary layer analysis that includes significant combustion case gas and small vena contracta laminar cooling-turbulent mixing effects. Experimental 1320 K chromium plate recrystallization temperature depths and 1000 K gun steel transformation temperature depths are used to calibrate these improved boundary layer analyses.

Combustible case gases are approximately 1600 K maximum for the M829 and M829A2 rounds while their respective propellant core flow gases are approximately 3000 K and 3300 K maximum. This combustible case ablates and its cooler gases (compared to the core flow) stay along the wall providing a laminar cooled boundary layer from the 0.6 meter RFT onset of the bore to where it changes over to fully turbulent in the 1.2-2.4 meter RFT region. This laminar cooling reduces heat transfer to the wall and diminishes with increasing axial position. The laminar to turbulent boundary layer transition is due to geometry and flow field conditions that are characterized by a transition from well-behaved streamlines with microscopic fluid mixing to loss of well-behaved streamlines with macroscopic fluid mixing.

Chamber-forcing cone-bore geometry of the M256 gun and its M829 and M829A2 rounds induce a vena contracta flow from the 0.6 meter RFT onset of the bore to the 1.2-2.4 meter RFT region. This type of flow exhibits slightly slower velocities between its streamlines and the wall which slightly reduce heat transfer to the wall and diminish with increasing axial position.

Without these combustion case gas laminar cooling and vena-contracta laminar cooling effects, the 0.6-1.2-meter region would be the highest wall heat transfer region. With both these laminar-cooling effects, the 1.2- 2.4-meter region is the highest wall heat transfer region since turbulence mixing in the boundary layer greatly diminishes these laminar-cooling effects after the approximate 1.2-meter transition point.

Improved boundary layer analyses are similar to transpiration, slot injection, and pure fuel injection cooling at the wall for rocket chambers as well as ablative cooling at the wall in guns.

For M256 gun tube #1988, Figure 3 summarizes the CCET thermochemical analyses of reacting wall enthalpy (Hw) and ablation potential (Ba) for the M829 and M829A2 rounds as a function of wall materials (HC chromium plate, A723-iron substrate) and wall temperature (Tw). Selected axial positions and round conditioning temperatures are the same as those in Figure 1. Experimental kinetic rate function data and subsurface metallographic data are used to calibrate the thermochemical analyses and transform the chemical equilibrium analyses into a partial chemical kinetic analyses. The respective HC chromium maximum Tw's are about 1600 K and 1650 K for the M829 and M829A2 rounds. These chromium Tw's are below their passivating oxidation temperature at about 2000 K and well below its melting point at about 2130 K which explains their inertness. The respective A723-iron maximum Tw's are about 1375 K and 1400 K for the M829 and M829A2 rounds. These A723-iron Tw's are well above its rapid expansive flaking oxidation temperature at about 1055 K, below its iron oxide melting point at about 1640 K, and well below its A723-iron melting point at about 1810 K which explains its reactivity.

For M256 tube #1988, Figure 4 summarizes the borescope data analysis of the A723 subsurface exposure through HC chromium plate cracks for the M829 and M829A2 rounds as a function of rounds fired and axial position. Selected axial positions and round conditioning temperatures are the same as those in Figure 1. This experimental borescope data is used to calibrate the erosion analysis and it was collected on a cleaned M256 tube that had about half M829A2 and half M829 rounds. These M829A2 and M829 rounds consisted of a nearly equal distribution of hot, ambient, and cold temperature conditioning. Data collection involves the use of a magnifying bore scope with a calibrated scale to measure the number and average area of each HC chromium platelet within a designated total area as a function of axial position for a given round count.

We were able to collect high quality borescope data on a single M256 tube with approximately half M829 and half M829A2 rounds near its 50 round point, near its 150 round point, and at its final out-of-service round point. The initial zero round condition data was not collected from this M256 tube but from the many unfired M256 tubes available at the Watervliet Arsenal. HC chromium plate has fine cracking and finite shrinkage when manufactured prior to firing. To date, it has been a difficult feat to collect in-service M256/M829Ax series borescope data and then continue to follow that tube until it is taken out of service. Regarding tube #1988 borescope data, we recognize that this is a sample of one and that significant variability exists depending on combinations of round count, round type, round conditioning temperature, and their round order. The borescope data in Figure 4 was verified by subsurface metallographic analysis for this out-of-service M256 tube.

For the 0.69, 1.55, 2.18, and 3.30 meter RFT axial positions in Figure 4, A723 subsurface exposure rapidly rises from about 50-125 rounds due to HC chromium non-metallic outgassing and compression resulting in its shrinkage and heat checking. After about 125 rounds, the A723 subsurface exposure rises slower due to a HC chromium platelet spalling mechanism. In Figure 4 for the 5.11 meter RFT near muzzle position, A723 subsurface exposure rises very rapidly from about 125 rounds until its out-of-service round count due to HC chromium platelet spalling by a different purely mechanical mechanism. Severe muzzle wear is likely responsible for removing this M256 tube from service at about seventy percent of its erosion life.

For M256 tube #1988, Figure 5 presents two typical 100x metallographs of a M256 tube with about half M829A2 and half M829 rounds at 0.69 meters RFT representing the 0.6-1.2 meter region. This 0.6-1.2 meter region has the highest gas pressure of any bore region (Figure 1) which explains the deep crack depths due to severe dilation. Although this 0.6-1.2 meter region has the highest gas temperature of any bore region (Figure 1), heat transfer to the wall is significantly diminished due to combustion case gas and vena contracta laminar cooling-turbulent mixing effects (Figure 2). These observations explain the heat checking and crack spacing as well as the near absence of interface degradation and chromium platelet spalling.

For M256 tube #1988, Figure 6 presents two typical 100x metallographs of a M256 tube with about half M829A2 and half M829 rounds at 1.55 meters RFT representing the 1.2-2.4 meter region. This 1.2-2.4 meter region has a lower gas pressure than the 0.6-1.2 meter region (Figure 1) which explains the

moderate crack depths due to moderate dilation. Although this 1.2-2.4 meter region has a lower gas temperature than the 0.6-1.2 meter bore region (Figure 1), heat transfer to the wall is significantly higher due to turbulent mixing of the combustion case gas and cessation of vena contracta effects (Figure 2). These observations explain the heat checking and crack spacing as well as the prevalent interface degradation and chromium platelet spalling. The erosion mechanism consists of heat checking of the inert chromium plate, subsequent interfacial degradation of the subsurface gun steel substrate at the chromium crack bases, subsequent chromium platelet spalling, and subsequent bare gun steel gas wash. As chromium platelets detach from the substrate and rise above attached chromium platelets, they are more susceptible to mechanical removal by the projectile. Rarely do heat checking cracks link-up to spall a chromium platelet with attached gun steel.

For Figures 5 and 6, experimental 1320 K chromium plate recrystallization temperature depths and 1000 K gun steel transformation temperature depths are used to calibrate calculated wall temperature profiles as a function of axial position.

Figure 7 summarizes the 120mm M256 gun tube serial number 1988's distribution of round types (M829, M829A2) and round conditioning temperatures (hot, ambient, cold) which are the same as those in Figure 1.

For tube #1988, Figure 8 summarizes the MACE material-ablation-conduction-erosion analyses for HC chromium maximum surface temperature (Tw) as a function of axial position, round type, and round conditioning temperature. Selected axial positions, round types, and round conditioning temperatures are the same as those in Figure 1. The respective HC chromium maximum Tw's are about 1600 K and 1650 K for the M829 and M829A2 rounds. These chromium Tw's are below its passivating oxidation temperature at about 2000 K and well below its melting point at about 2130 K which explains its inertness. In Figure 8, experimental 1320 K chromium-plate-recrystallization-temperature depths as a function of axial position calibrate calculated wall temperature profiles.

For tube #1988, Figure 9 summarizes the MACE material-ablation-conduction-erosion analyses for A723 maximum interface and surface wall temperatures (Tw) as a function of axial position, round type, and round conditioning temperature. Selected axial positions, round types, and round conditioning temperatures are the same as those in Figure 1. These respective A723-iron maximum interface Tw's are about 1225 K to 1250 K for the M829 and M829A2 rounds. The respective A723-iron maximum surface Tw's are about 1375 K and 1400 K for the M829 and M829A2 rounds. These A723-iron Tw's are above its rapid expansive flaking oxidation temperature at about 1055 K, below its iron oxide melting point at about 1640 K, and well below its A723-iron melting point at about 1810 K which explains its reactivity. Diffusion, reactions, and gas wash thermochemically degrade interfacial A723 at HC chromium plate heat checked crack bases and also fully exposed A723 after HC chromium plate spalling. In Figure 9, experimental 1000 K A723-transformation-temperature depths as a function of axial position calibrate calculated wall temperature profiles.

For Figures 8-9, wall temperature profiles follow the heat transfer pattern from Figure 2, where these wall temperatures increase with increasing axial position for the 0.6-1.2 meter RFT region, peak in the 1.2-2.4 meter range, then decrease with increasing axial position to the muzzle. Again, this is due to combustion case gas and vena contracta laminar cooling-turbulent mixing effects.

For 120mm M256 gun tube serial number 1988, Figure 10 summarizes the MACE material-ablation-conduction-erosion analyses for the cumulative erosion as a function of cumulative rounds and axial position. Selected axial positions, round types, and round conditioning temperatures are the same as in Figure 1. Tube #1988 was taken out-of-service by dispersion at 424-rounds which is about seventy percent of its estimated erosion life. In Figure 10, the 2.18-meter RFT axial position is the most eroded position and has approximately 3mm of cumulative erosion at 424 rounds. If this gun tube remained in service, it should last an estimated 550 to 600 rounds before it was condemned by erosion at 5-mm depth. The 2.18-meter position takes about 170 rounds for chromium platelet spalling onset and A723 gas wash onset to occur.

For Figure 10, cumulative wall erosion profiles follow the heat transfer pattern from Figure 2. This pattern includes the increase of cumulative wall erosion with increasing axial position for the 0.6-1.2 meter RFT region, the peaking of cumulative wall erosion in the 1.2-2.4 meter range, then the decrease of cumulative wall erosion with increasing axial

position to the muzzle. Again, this is due to combustion case gas and vena contracta laminar cooling-turbulent mixing effects. Erosion life is lowest at the 2.18-meter, higher at 1.55-meter, still higher at 0.69-meter, higher yet at 3.30-meter, and highest at 5.11-meter. These four Figures show that interface life follows the same pattern with the exception of the 5.11-meter position.

Also for Figures 10, the erosion mechanism consists of heat checking of the inert chromium plate, subsequent interfacial degradation of the subsurface gun steel substrate at the chromium crack bases, subsequent chromium platelet spalling, and subsequent bare gun steel gas wash. Mechanisms of interface degradation include diffusion, reactions, and gas wash. For example, sufficient iron oxidation formed at the chromium/A723 interface occupies a larger volume than the original iron and pushes up the chromium platelet leading to eventual chromium platelet spalling. This overall 120mm M256 gun tube serial number 1988 gun erosion analysis correctly predicts that the worst eroded region is at 1.2 – 2.4 meters RFT and that the excessive muzzle wear at 5.11 m (chromium loss without gun steel gas wash) is by a different purely mechanical mechanism.

REFERENCES

1. Alkidas, A., Morris, S., Christoe, C., Caveny, L., and Summerfield, M., "Erosive Effects of Various Pure and Combustion-Generated Gases on Metals - Part II," US Army Materials and Mechanics Research Center Technical Report, Watertown, MA, 1977; see also Part I, 1975.

2. Picard, J., Ahmad, I., and Bracuti, A., Proceedings of the Tri-Service Gun Tube Wear and Erosion Symposiums, US Army ARDEC/ADPA, Dover, NJ, 1970, 1972, 1977, and 1982.

3. Dunn, S., Sopok, S., Coats, D., O'Hara, P., Nickerson, G., and Pflegl, G., "Unified Computer Model For Predicting Thermochemical Erosion In Gun Barrels," Proceedings of 31st AIAA Propulsion Meeting, San Diego, CA, July, 1995.

4. Gough, P., "The XNOVAKTC Code," Paul Gough Associates, Portsmouth, NH, 1990.

Fig 1 - NOVA Tube #1988 Max Pg, Tg & Vg

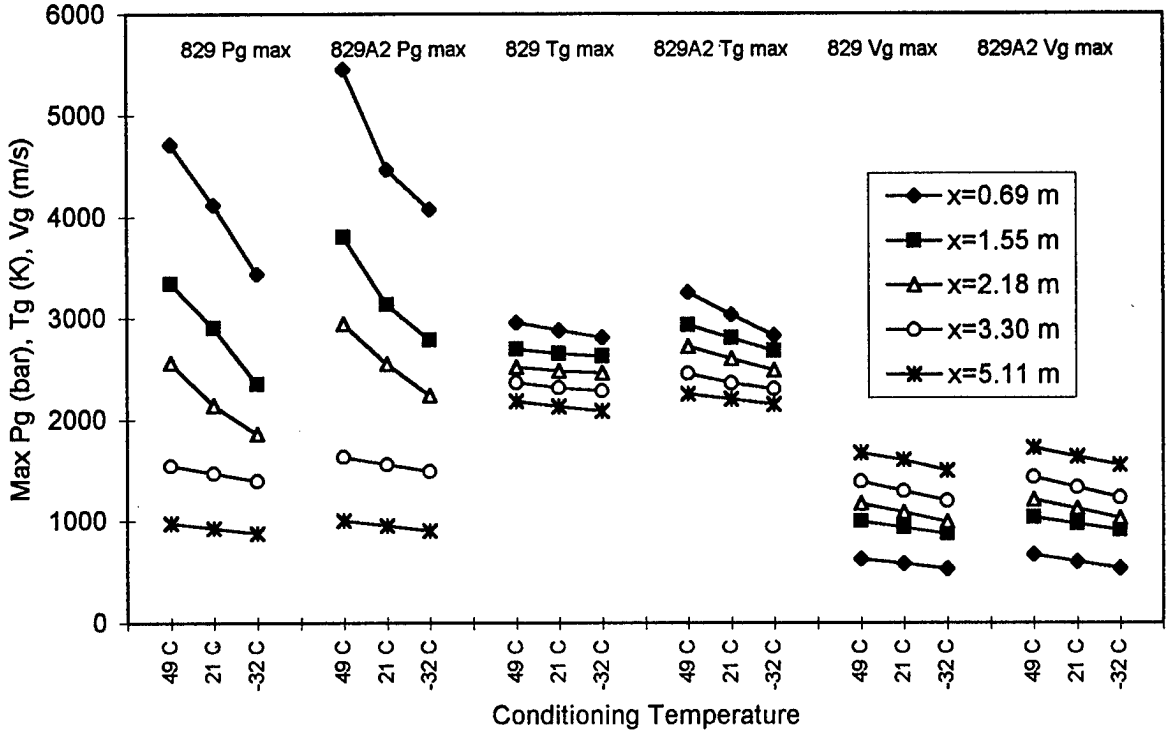

Fig 2 - MABL Tube #1988 Max Hr & Qcw

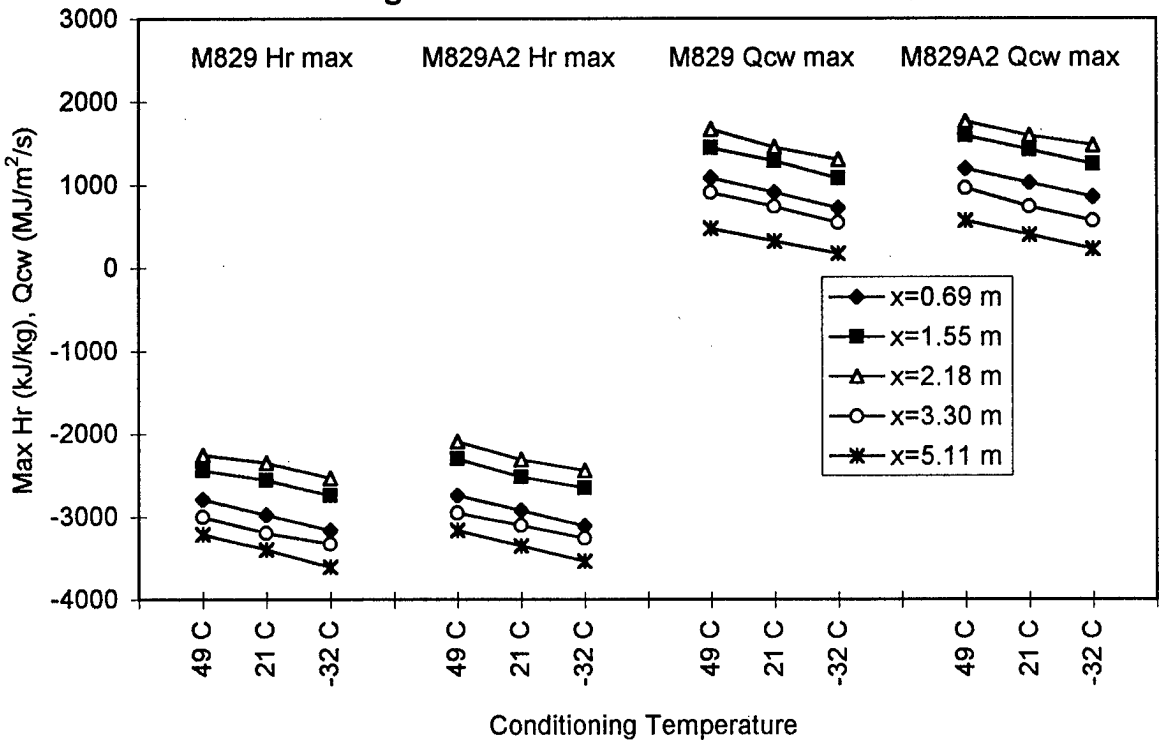

Fig 3 - CCET Tube #1988 Hw & Ba

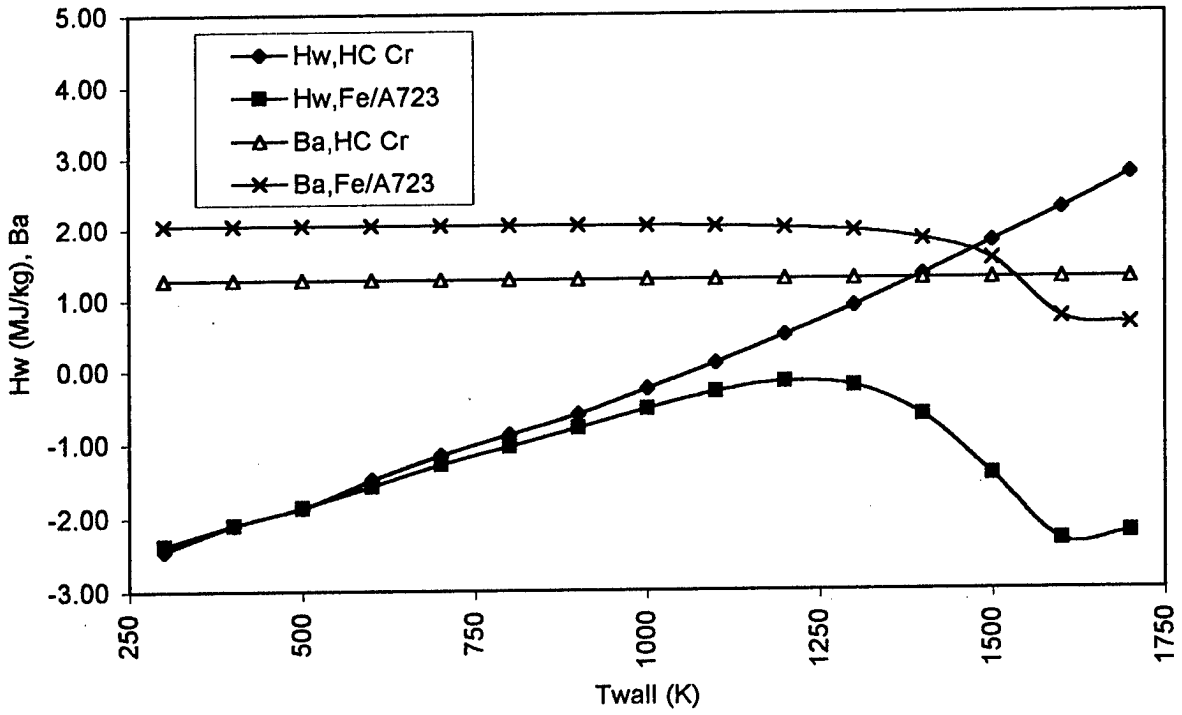

Fig 4 - Tube #1988 A723 Subsurf Exposure Borescope Data

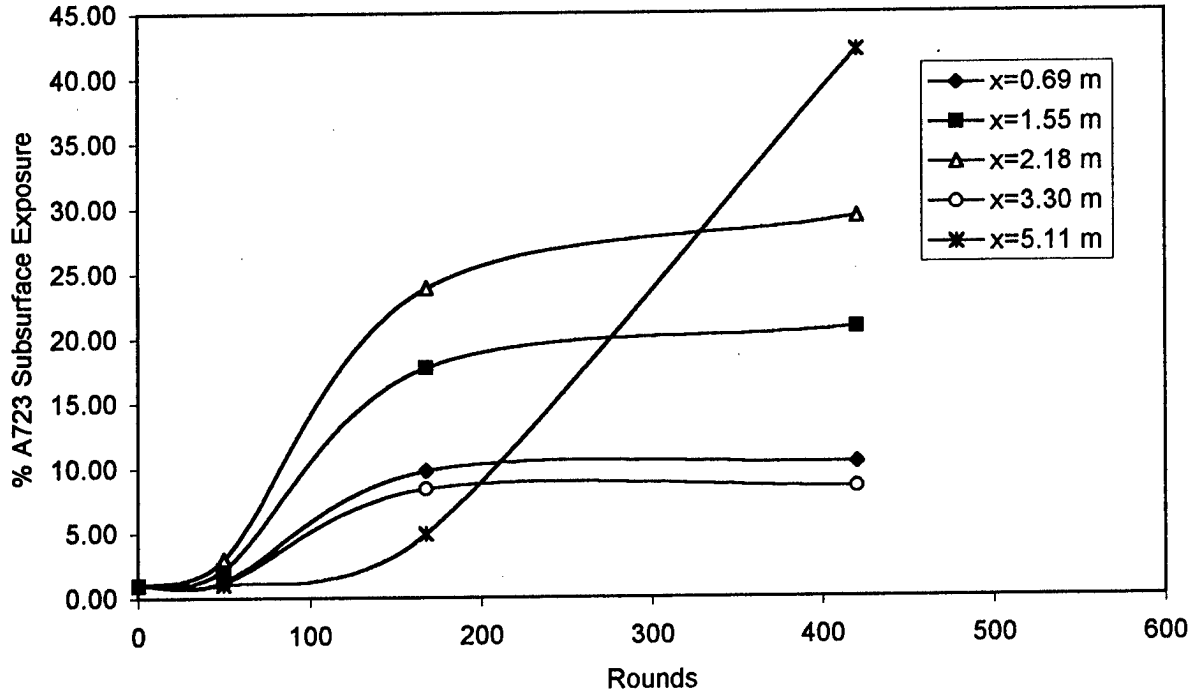

Fig 5 - Tube #1988 Metallographs At 0.69 m Representing 0.6-1.2 m Region

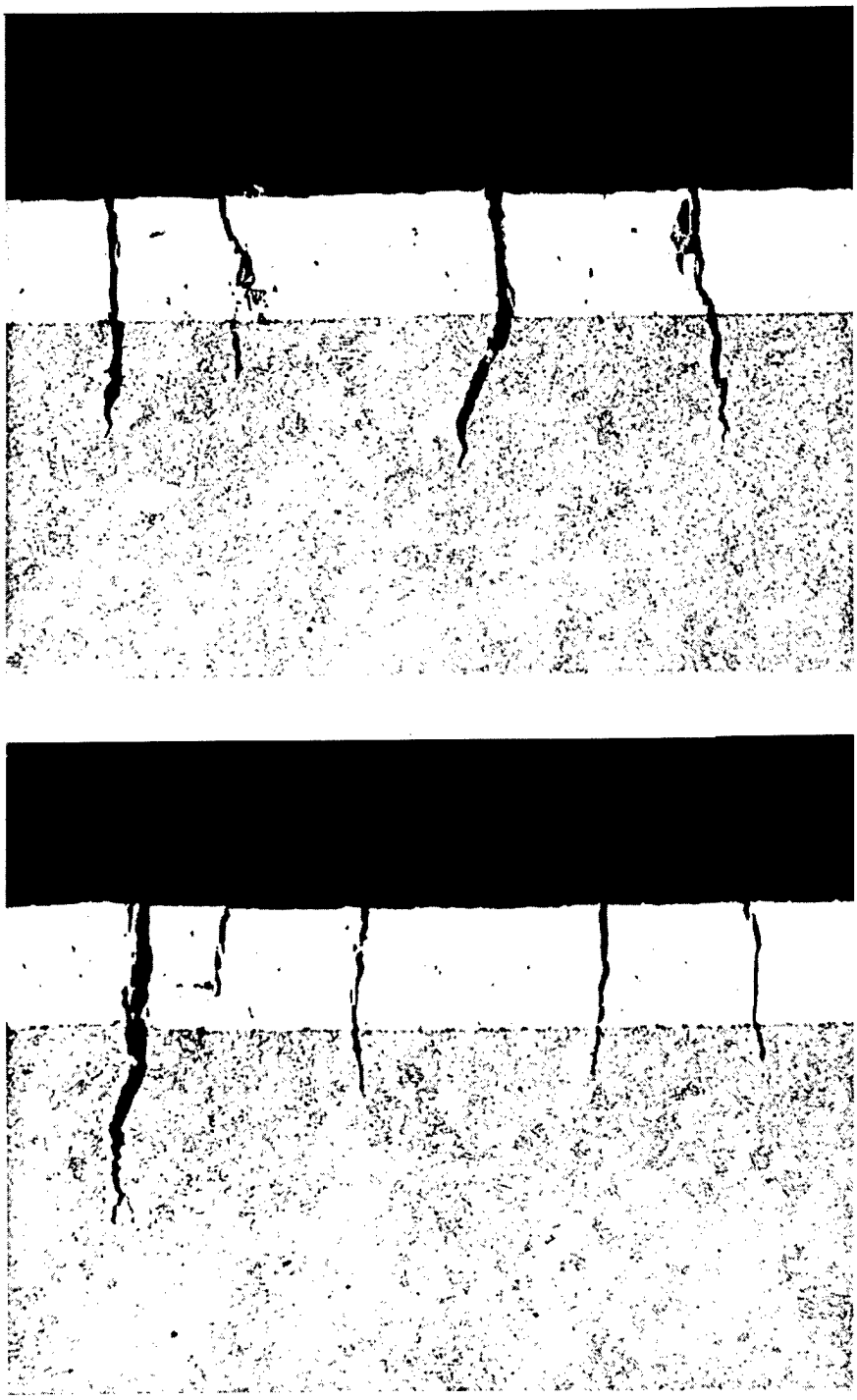

Fig 6 - Tube #1988 Metallographs At 1.55 m Representing 1.2-2.4 m Region

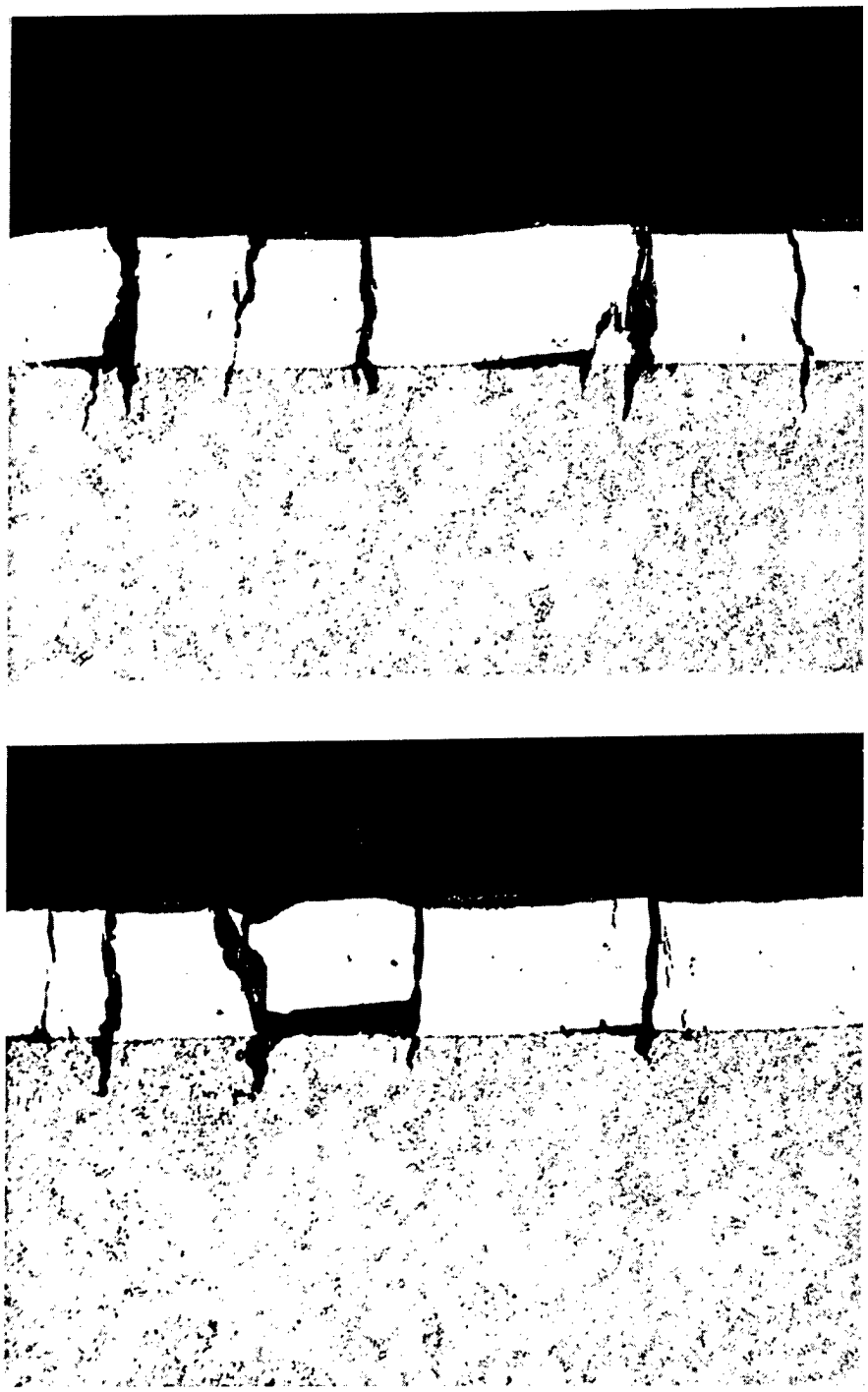

Fig 7 - Tube #1988 424 Round Distribution

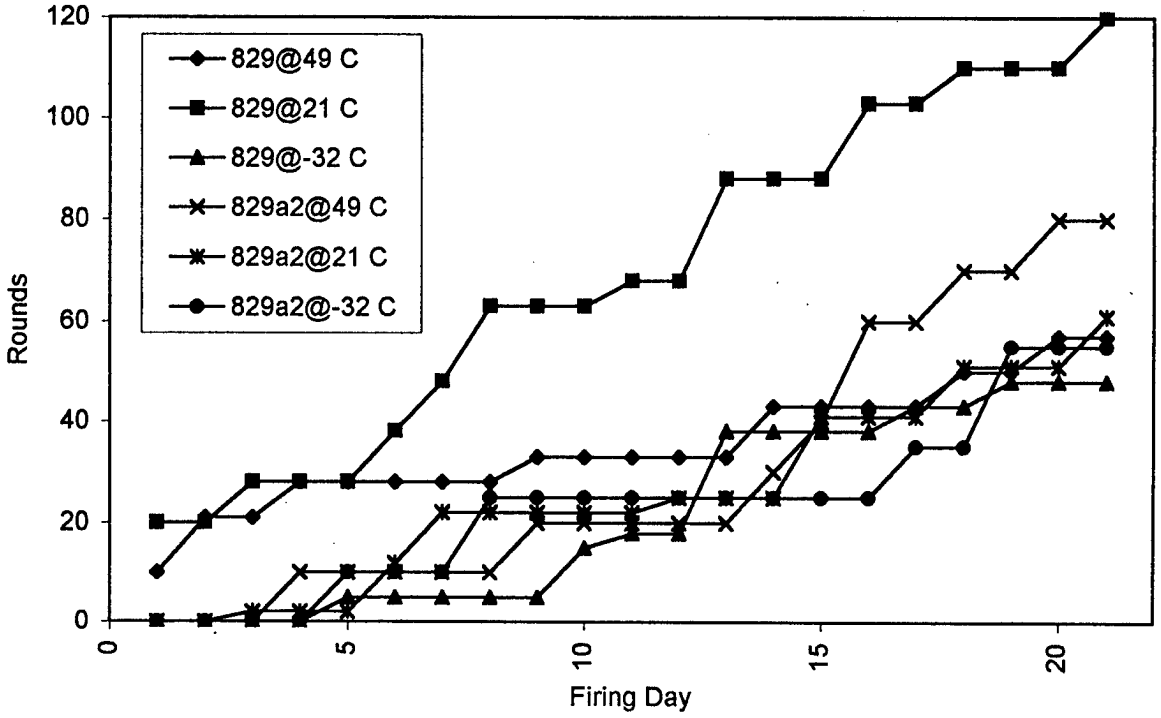

Fig 8-MACE Tube #1988 Max HC Cr Surface Tw

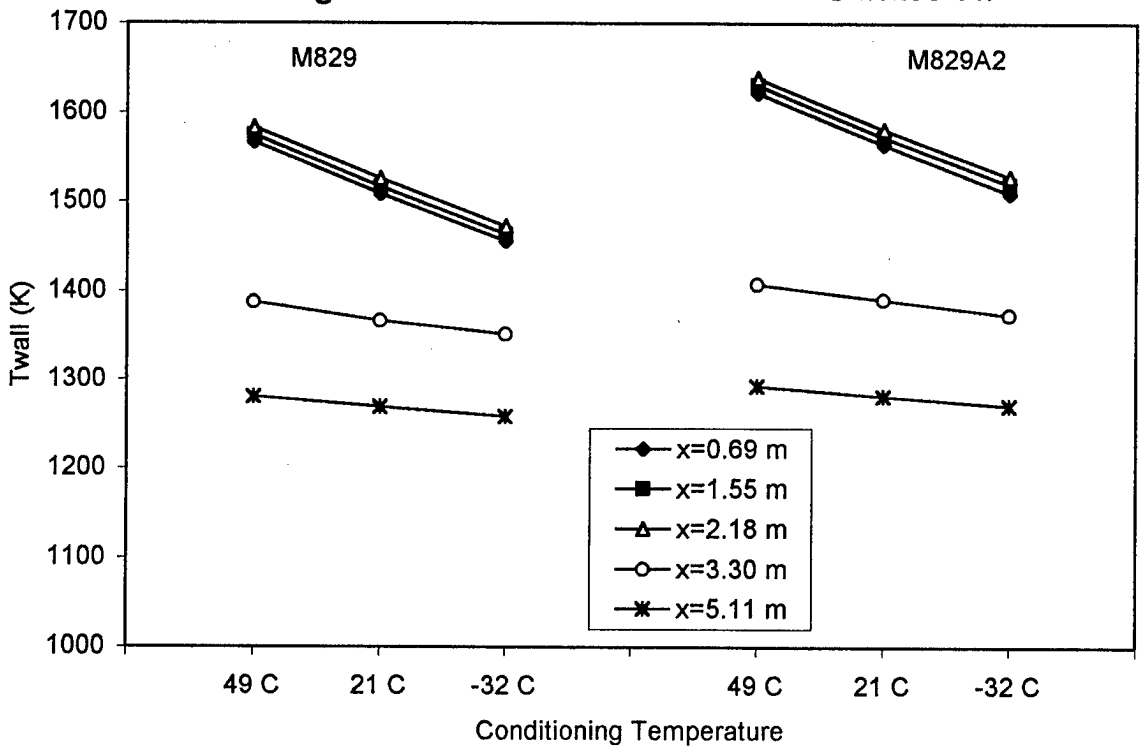

Fig 9 - MACE Tube #1988 Max A723 Tw

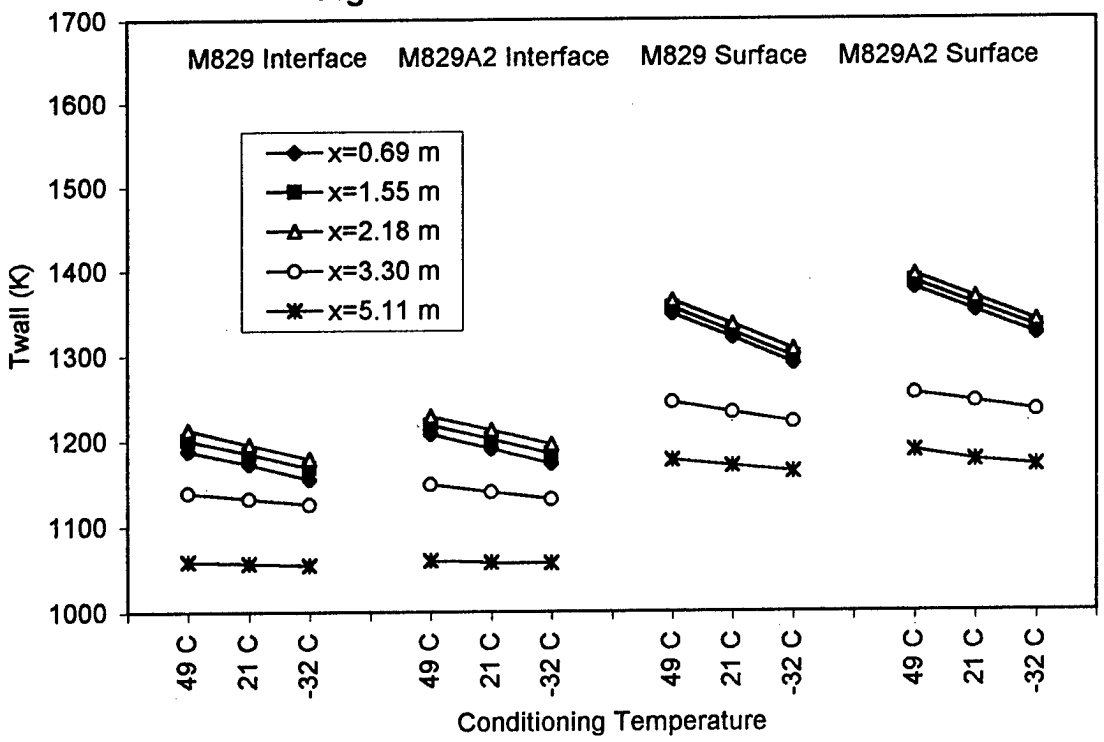

Fig 10 - MACE Tube #1988 Cumulative Erosion